X-Ray Tomography

AG Seemann

AG Seemann

January 18, 2024

This experiment gives you insights into fundamental properties of X-rays, their generation and interaction with matter as well as the use of X-rays in computerized tomography. The fundamental principle in this non-destructive imaging method is the material-dependent attenuation of X-rays from an ideally point-like X-ray source employed to aquire absorption transmission images of an object for a large number of different viewing angles and to compute the three-dimensional distribution of materials in the object. In this experiment, the generation of Bremsstrahlung in the X-ray tube and the dependence of the radiation intensity on the anode voltage and current is experimentally examined. The results are compared to the predictions based on Kramer's rule. Using wedges of different materials, Lambert-Beer's law is checked, which predicts and exponential decrease of X-ray intensity with the length of the transmission path. In addition, at the end of the experiment you are given the possibility to scan a suitable object of your choice and to create a three-dimensional tomography image.

CONTENTS

PREPARATION QUESTIONS

Read the instructions carefully and answer the following questions. The answer to these questions is part of the Antestat colloquium. The questions also serve as 'guidelines' for the theoretical foundations section of your elaboration.

Task 1: Summarize the basic findings about X-rays that Wilhelm Conrad von Röntgen formulated in his first publication "*About a new type of rays (Preliminary communication)*" from 1895, e.g. via Wikisource).

Task 2: Explain the formation of X-ray Bremsstrahlung and characteristic X-rays and describe the generation of X-rays in a synchrotron and in a X-ray tube.

Task 3: Sketch the X-ray spectrum for a typical anode material of your choice. Classify X-rays in the electromagnetic spectrum.

Task 4: When do the X-ray photons produced in a X-ray tube carry the maximum possible energy? Provide an expression for the maximum photon energy $E_{\max}$ and the corresponding minimum wavelength.

Task 5: Sketch the intensity of the X-rays as a function of the wavelength according to Kramer's rule and, by integrating equation 1.4, justify what type of dependence you expect for the total intensity of the X-rays as a function of the acceleration voltage U or the anode current I.

Task 6: Name and explain the different types of interaction when X-rays pass through a medium and assign typical photon energies to each type of interaction. Which of these processes are dominant for the X-ray energy range relevant in this experiment?

Task 7: Describe qualitatively how a variation of the X-ray parameters acceleration voltage, anode current and integration time affects the image recorded with the detector.

Task 8: Formulate Lambert-Beer's law and illustrate it with the help of a sketch.

Task 9: Explain the terms radiogram, tomogram and tomography and describe how a tomography is created.

Additional task: Select your own sample that you would like to view in the computer tomograph and bring it to the lab the day you carry out the experiment. The sample should be maximally the size of a fist and consist of materials with varying degrees of attenuation (i.e. no solid, fist-sized metal objects).

1. Theoretical Foundations

Discovered by the German physicist Wilhelm Conrad Röntgen in 1895, X-rays are a special type of electromagnetic Radiation, the properties of which were already discovered in the 19th century. Until today X-rays play an important role in fundamental and applied research like in material science and in the medical sector. In 1901 Wilhelm Conrad Röntgen received the first Nobel Prize in Physics for the discovery of what he called "X-rays". The term "Roentgenstrahlung", which is commonly used in German-speaking countries, only became established after Roentgen's death in 1923.

1.1. Generation of X-rays

X-rays like generally any other type of electromagnetic radiation are emitted by accelerated electric charges. Both the acceleration's magnitude and time dependence determine the spectral distribution of the emitted radiation. Collective oscillations of free charges in the antenna of a radio station, for example, generate radio waves; the much faster oscillations of electrons in the shell of an atom create visible light. Extremely fast charge oscillations in atomic nuclei lead to the emission of γ-radiation. With X-rays, that is electromagnetic radiation with a frequency above that of ultraviolet light (but below the typical frequencies of γ-radiation), a distinction is made between continuous Bremsstrahlung and discrete characteristic radiation depending on the type of its generation. X-rays of high intensity can be generated in a synchrotron. For applications requiring only low intensity radiation usually commercially available X-ray tubes are used. The mechanisms operating in each of the two devices, leading to the the emission of X-rays are examined in more detail below.

1.1.1. Synchrotron

Electrons travelling on a curved path at velocities slightly below the speed of light emit x-rays tangential to their path. This so-called Bremsstrahlung has a continuous spectrum, since the kinetic energy of the electrons is transferred in whole or in part to a X-ray photon. [1] This type of generation of X-rays is used in large synchrotrons, for example, at the ESRF in Grenoble, BESSY in Berlin, at DESY in Hamburg and many other research facilities around the globe. At the ESRF in Grenoble, for example, pre-accelerated electron bunches are inserted into an 844 m long storage ring and held on a circular path by magnets. At the ESRF, X-rays are generated in 32 straight and 32 curved sections of the storage ring (see Fig. 1.1).

In the curved sections, so-called *bending magnets* keep the electrons on their curved path. As a "by-product", X-rays with low brilliance are emitted that can be already used for applications with less demanding requirements. In the straight sections, magnets focus the electron beam before it enters a series of magnets with an alternating field called *wigglers* to create an high intensity X-ray beam. For example, the *n* wiggler magnets produce an *n* times higher intensity while the energy of the emitted X-rays depends on the distance between the magnets.

---

[1] In the following we will use the term "X-ray photon" and "X-ray quantum" synonymously.
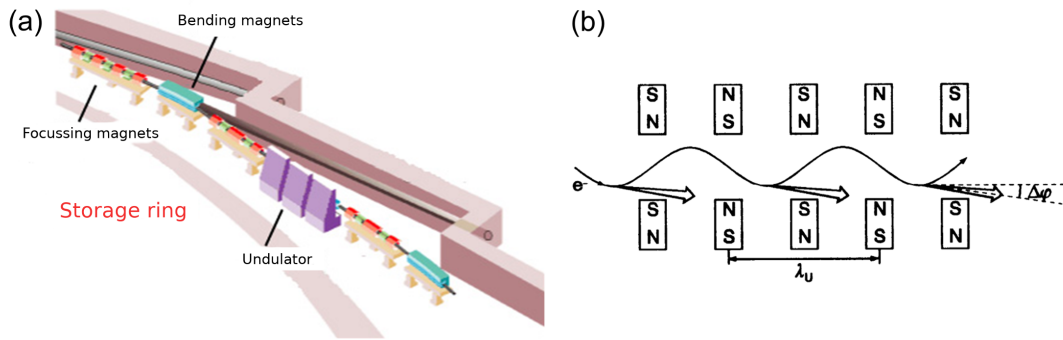
Figure 1.1: (a) Representation of a section of the storage ring at the ESRF in Grenoble to illustrate the different magnets that are needed to generate X-rays (source: wwww.esrf.eu). (b) Schematic representation of an arrangement of wigglers according to Ref. Kuzmany.

If the number of magnets is very large (on the order of 100), coherent radiation occurs due to interference in certain directions and at certain wavelengths. The peak intensity is then proportional to n^2. Such a sequence of alternating magnets is called an *undulator* (wave maker).

1.1.2. X-RAY TUBE

In many lab-scale applications, X-rays are produced with commercially available X-ray tubes. As illustrated in the schematic representation in Fig. 1.2, free electrons are generated in an evacuated tube by glow emission from a cathode which are then accelerated towards the anode by a voltage U applied between the cathode and the anode. The time it hits the anode, an electron with charge e carries the kinetic energy $E = eU$.
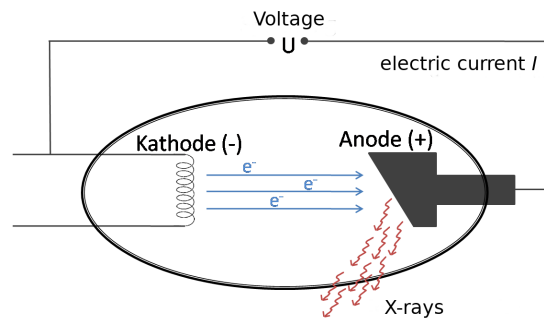

Figure 1.2: Schematic representation of a conventional X-ray tube for generating X-rays.

As a result of the interaction between the high energy electrons with the anode atoms, two different types of X-rays are generated: continuous radiation and characteristic radiation (see Fig. 1.3(a)). Once a fast electron enters the Coulomb field of a heavy atomic nucleus of the
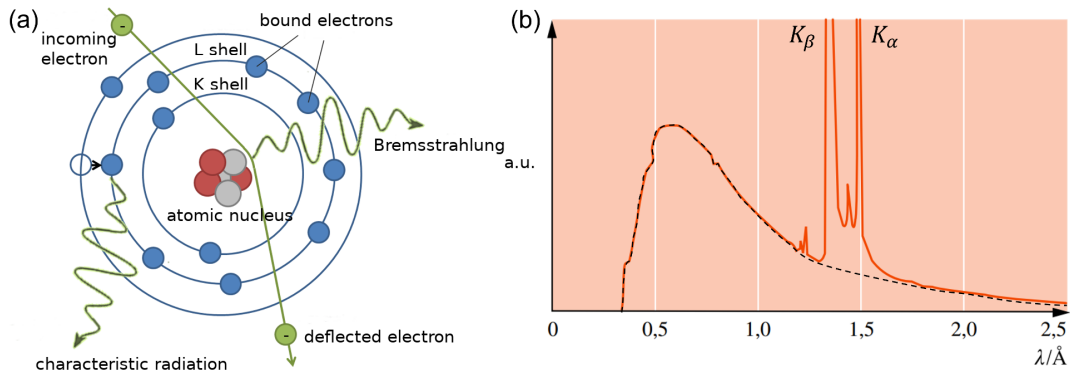
Figure 1.3: (a) Schematic representation of the formation of x-ray Bremsstrahlung and characteristic x-rays in the shell model. (b) x-ray spectrum of a copper anode for a tube voltage of 38 kV displaying continuous Bremsstrahlung (dotted line) and superimposed K_α and K_β lines (source: Gerthsen Physics [1]).

anode material, for example tungsten, it is deflected from its initial direction of motion and emits *Bremsstrahlung* which contributes to the continuous spectrum.

If the accelerated electron collides with the shell electrons of the atoms in the anode, so-called *characteristic radiation* is created. If the energy of the fast electrons in the X-ray tube is high enough, they can kick out tightly bound electrons from energetically low shells during the collision. Atoms of the anode material excited in this way relax through the emission of X-ray photons: Electrons from outer shells fill the vacated holes and thereby emit radiation with a wavelength that is characteristic of this transition. Non-radiative relaxation processes are also possible: while an electron of a higher energy level fills the vacated hole, the released energy is transferred to an outer electron which is emitted (Auger-Meitner effect).

The spectrum of a x-ray tube therefore consists of a continuous part and a characteristic part with intensity maxima being specific for the material of the anode. The continuously distributed part of x-rays is limited to short Wavelengths of the spectrum through the minimum wavelength:

$$\lambda_{\min} = \frac{h\,c}{e\,U}\,,\tag{1.1}$$

since the maximum photon energy corresponds to the kinetic energy of the electrons $E_{\max} = e \cdot U$. This cutoff wavelength does not depend on the type of anode material and is determined solely by the kinetic energy of the electrons, i.e. the acceleration voltage. Named after its discoverers, equation 1.1 is called the law of Duane-Hunt. In Fig. 1.3(b) the x-ray spectrum of a copper anode is shown as an example.

The wavelength of the characteristic emission lines follows the law of Moseley. For the frequency of the photons of the K_α line, which is emitted during the transition of an L-shell electron into the K-shell, the following equation applies:

$$\lambda_{K_\alpha} = \frac{3\,c}{4\,R_\infty (Z-1)^2}\tag{1.2}$$

where m_e is the electron mass, Z the atomic number and $R_\infty = m_e\,e^4/8\,c\,\varepsilon_0\,h^3 = 3.290{\cdot}10^{15}$ Hz the Rydberg frequency. The wavelengths of characteristic X-ray photons of heavy elements with high atomic number follow the same law describing the wavelength of photons emitted by excited hydrogen atoms (the Lyman α-line). The factor $(Z-1)^2$ takes into account the screening of the nuclear charge by the remaining electron in the K-shell.

1.1.3. INTENSITY DISTRIBUTION

A first theoretical investigation into the generation of the continuous spectrum of X-rays is the work of Kramers [2]. This theory predicts a linear decrease in the intensity of X-rays with frequency ν. The intensity vanishes at a limit frequency $\nu_{\max} = c/\lambda_{\min}$. The intensity distribution proposed by H.A. Kramers has the form [2]:

$$\mathrm{d}J_\nu(\nu) = K\,I\,Z\,(\nu_{\max} - \nu)\,\mathrm{d}\nu\,, \tag{1.3}$$

where $\mathrm{d}J_\nu(\nu)$ is the radiant energy per time and frequency interval $\mathrm{d}\nu$ represents emitted in all spatial directions , while I is the strength of the anode current and Z the Atomic number of the anode material. Kramer's constant K depends on the geometry of the anode.

To describe the intensity of X-rays, the representation $J_\lambda(\lambda)$ in wavelength space has been established. Employing the differential relation $|\mathrm{d}\nu| = c\lambda^{-2}|\mathrm{d}\lambda|$ equation 1.3 yields:

$$\mathrm{d}J_\lambda(\lambda) = \frac{c^2 K\,I\,Z}{\lambda^2}\left(\frac{1}{\lambda_{\min}} - \frac{1}{\lambda}\right)\mathrm{d}\lambda\,. \tag{1.4}$$

Integrating equation 1.4 between $\lambda_{\min}$ and ∞, as well as inserting the expression 1.1 for the wavelength $\lambda_{\min}$ gives an expression for the total intensity of the X-rays as function of acceleration voltage U and anode current I (Ulrey's law):

$$J_{\mathrm{ges}} \propto I\,U^2\,. \tag{1.5}$$

You will check this dependency in chapter 6.2 also experimentally.

1.2. ATTENUATION OF X-RAYS IN MATTER

When passing through a gas, liquid or solid, X-ray photons interact with matter so that the X-ray is attenuated. On the one hand, this happens through absorption of the x-ray photons as well as by the scattering of the x-ray photons into different directions.

- In the *photo effect*, the incoming x-ray photon is absorbed by a strongly bound electron, which is released from its bound state due to the supplied energy. The photon is destroyed in this process, with the excess photon energy becoming the kinetic energy of the released electron.

- In *Thomson* or *Rayleigh scattering* the photon is elastically scattered by bound electrons of the atomic shells. The energy of the incident and scattered photon are identical. Since in an elastic scattering process the scattered Photons can interfere depending on the scattering angle, the intensity is related to the electron density in the atomic lattice.

- In the *Compton effect*, the incoming photon collides inelastically with a weakly bound electron in the atomic shell. In contrast to the elastic Thomson or Rayleigh scattering, part of the photon energy is transferred to the electron during the collision and the inelastically scattered photons cannot interfere.

- If a single X-ray photon has an energy $E > 1.022\,\text{MeV}$, *pair generation* can occur in the presence of matter. The X-ray photon creates an electron-positron pair, with both particles having a rest energy of $0.511\,\text{MeV}$. However, due to conservation of momentum, the creation of an electron-positron pair is only possible if momentum can be exchanged with another particle via a field. In heavy atoms, pair generation in the electric field of the atomic nucleus predominates over pair generation in the electric field of the shell electrons.

The relative contribution of the described processes to the attenuation of X-rays in matter depends on the energy of the incoming X-ray photons. In general, the attenuation coefficient μ is the product of the sum of all effective cross sections for scattering and absorption, σ, and the particle density n. The energy dependence of the effective cross sections for the above-mentioned processes is illustrated in Fig. 1.4 using lead as an example. The effective cross section of the photo effect increases with the energy of the X-ray photons: [2]:

$$\sigma_{\text{p.e.}} \propto \frac{Z^4}{E_\text{p}^3} \,.$$

(1.6)

If the energy of the x-ray photons E_p exceeds the ionization energy of an inner electron shell the cross section for absorption and scattering increases discontinuously. The resulting edges in the attenuation spectrum can be clearly seen in Fig. 1.4.

For x-ray energies up to about $500\,\text{keV}$ the photo effect contributes largely to the attenuation coefficient. The Compton effect dominates at x-ray energies up to about $5\,\text{MeV}$. At even higher energies, pair production is the major contribution to the attenuation coefficient μ. It is part of the preparatory questions to discuss the energy dependent contributions of the photo effect, the Compton effect and pair generation in respect to the total attenuation of X-rays in matter and to explain the three effects in detail.

Because of the energy dependence described above, the photo effect typically represents the dominant contribution to the total attenuation of X-rays for most of the in-house tomography setups where the maximum energy of the photons is limited to $< 200\,\text{kV}$.

The three-dimensional image generation in the computer tomograph is based on the fact that X-rays are attenuated to different extents in materials of different types or different thicknesses. The more photons are absorbed or scattered as they pass through a sample, the fewer X-ray photons arrive at the detector. The X-ray tomograph used in the experiment has a scintillation detector which is typically used in medical applications.

Some of the incident X-ray photons generate fast photoelectrons in the detector, which, in a cascade of processes, stimulate the atoms of the scintillator material to emit photons in the visible spectrum. The resulting secondary photons appear as flashes of light (scintiallations). The number of secondary photons is, in a first approximation, proportional to the energy of the absorbed X-ray photon, so that the number of secondary photons detected per time is a
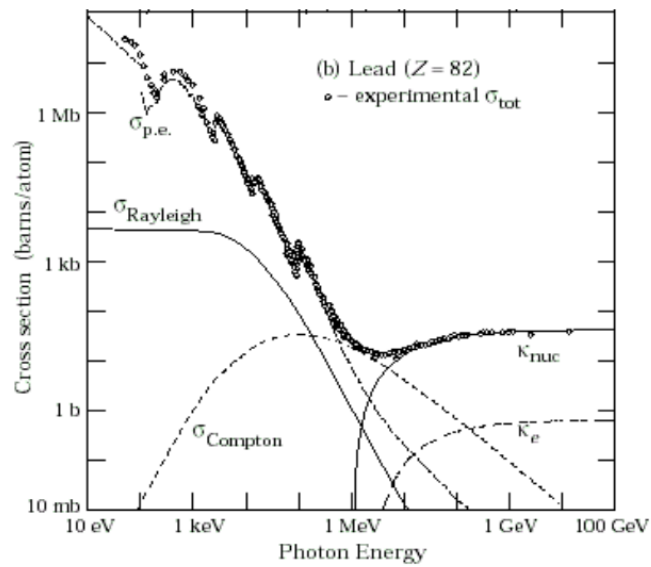
Figure 1.4: Cross sections of the processes that lead to an attenuation of the x-rays in matter: $\sigma_{\text{p.e.}}$ photo effect, σ_{Rayleigh} Thomson or Rayleigh scattering, σ_{Compton} Compton scattering, κ_{nuc} pair production in the nuclear field and κ_{e} pair production in the field of bound electrons. Source: http://physics.nist.gov/PhysRefData). One barn (b) equals $10^{-28}\text{m}^2 = (10\,\text{fm})^2$.
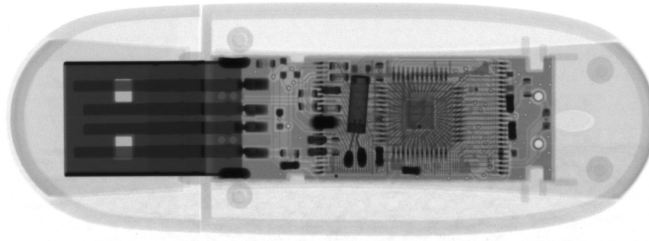
Figure 1.5: Radiogram of a USB key from Intenso with a plastic housing and metal components.
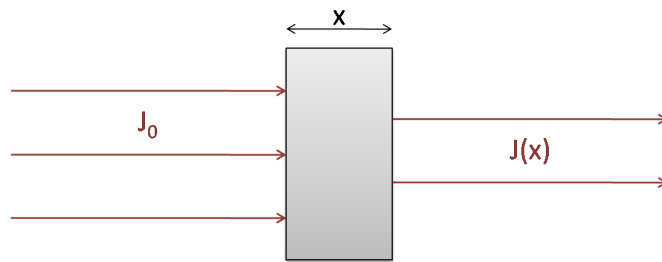

Figure 1.6: Schematic representation of the intensity $J(x)$ of X-rays attenuated when passing through a material of thickness x.

direct measure of the intensity of the X-ray radiation. Scintillator materials for imaging detectors usually contain elements with a high atomic number in order to achieve the greatest possible yield of photoelectrons.

A measure of the number of photons counted in a certain region of the detector is the so-called gray value, which is higher the more secondary photons are detected at this point. In the radiogram, the areas of greatest attenuation are shown with the lowest gray values and therefore appear darkest. Areas of low attenuation are represented by high gray values and appear bright. The thick plastic housing of the USB key can be penetrated by the X-rays almost unhindered and is displayed brightly, i.e. with high gray values, cf. the radiogram of a USB key in figure 1.5. The metallic components inside the USB key absorb large parts of the X-rays and appear dark on the radiogram, are therefore represented by low gray values.

1.2.1. LAMBERT-BEER LAW

The *Lambert-Beer absorption law* describes the attenuation of the X-rays within a sample, that is, the decrease in intensity J of an vertically incident, parallel x-rays beam after passing through a material of thickness x in comparison to the initial radiation intensity J_0 (see figure 1.6).

If N_0 X-ray photons of a given wavelength enter a thin layer of a material of thickness dx,

the number of photons changes by dN:

$$\mathrm{d}\tilde{N} = -\mu\,\tilde{N}\,\mathrm{d}\tilde{x}\,. \tag{1.7}$$

as the beam passes through the layer. Here μ is the energy dependent attenuation coefficient that comprises both absorption and scattering of the X-rays within the material. Integration of equation (1.7) leads to:

$$
\begin{aligned}
\int_{N_0}^{N} \frac{\mathrm{d}\tilde{N}}{\tilde{N}} &= \int_0^x -\mu\,\mathrm{d}\tilde{x} \\
\ln\left(\frac{N}{N_0}\right) &= -\mu\,x \\
N(x) &= N_0\,e^{-\mu x} \tag{1.8}
\end{aligned}
$$

Since number of photons N and intensity J of monochromatic radiation are proportional to each other, equation (1.8) gives the following expression for the intensity of monochromatic X-rays as a function the irradiated thickness x of the material:

$$J = J_0\,e^{-\mu x}\,. \tag{1.9}$$

In contrast to a beam of monochromatic x-rays with wavelength λ, the total intensity of a polychromatic x-ray beam as a function the thickness is a convolution of exponential functions with varying attenuations $\mu(\lambda)$. Qualitatively, the drop of the total intensity $J(x)$ becomes slower with increasing thickness x, because long-wave components of the X-ray beam are generally attenuated more strongly and are absorbed in the material after just a short distance. This means that the average wavelength of the intensity spectrum shifts to shorter wavelengths, i.e. a higher energy as the penetration depth increases. This shift towards "harder" x-rays is referred to in the literature as *beam hardening*.

2. EXPERIMENTAL SETUP

For the present experiment, a computer tomograph of the type "*CT-Alpha*" from *ProCon X-Ray* is used. The CT alpha is equipped with a 160 kV x-ray tube fitted into a lead-lined full protection cabin. From both long sides of the cabin, the interior of the CT-Alpha is accessible via a sliding door. Several closing contacts ensure that the X-ray tube can be put into operation only while the cabin is locked. Electric lines and tubes can be led into the interior of the CT through cable channels which are also secured by closing contacts. All components including the x-ray tube, the rotating sample table and its axes and the detctor are mounted on a granite slab to suppress vibrations and limit thermal expansion. The CT-Alpha is 180 cm long, 80 cm wide and 180 cm high and weighs approx. 2100 kg.
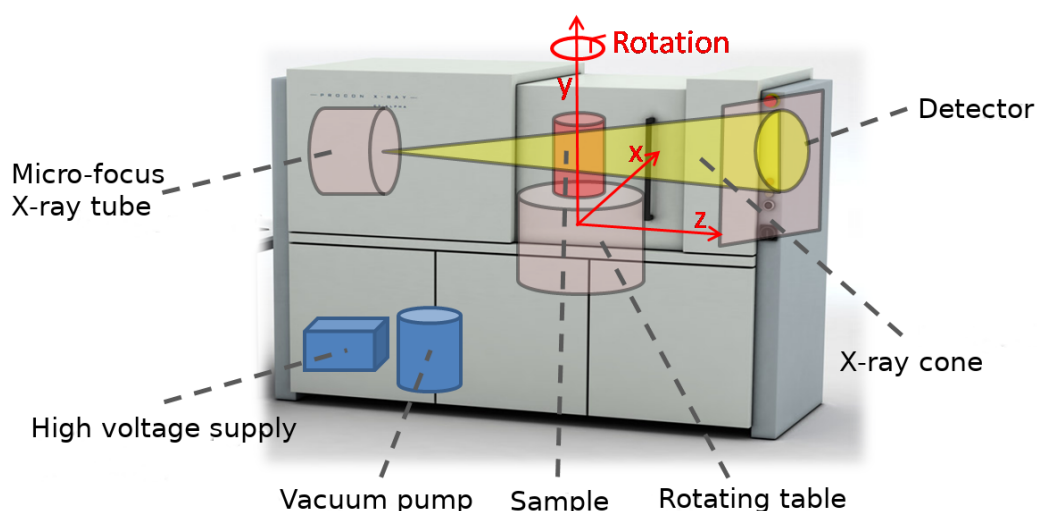

Figure 2.1: Schematic representation of the CT-Alpha computer tomograph. The position of the axes on which the sample table can be moved.

The sample table can be moved in all three spatial directions and also rotated around its own axis, see Fig. 2.1. The sample table can be placed along the 600 mm long Z-axis or magnification axis in minimum Increments of 100 μm, along the 100 mm long Y-axis or height axis with minimum increments of 1 μm and along the 30 mm long X-axis with minimum increments from 0.1 μm. The displacement speed is 1.5 mm/s. The sample stage can rotate by 360° at an angular speed of up to 45°/s. The too Samples to be examined may have a maximum diameter of 400 mm and a maximum height of 400 mm. The maximum sample weight is 10kg.

The X-rays are produced using a microfocus X-ray tube of the type 160-THE manufactured by the company X-Ray WorX. This tube uses anode voltages ranging between 10 kV and 160 kV. The operation parameters are limited to a **maximum power of 25 W**. The maximum anode current is limited to 1 mA for the lowest voltage dropping to a maximum of 0.05 mA for the highest voltage. The electron beam of the x-ray tube is focussed on a transmission target

made of a thin layer of tungsten on a diamond window. Tungsten has a high atomic number ($Z = 74$) and melting temperature ($T = 3422°$C), while diamond is a very good heat conductor and has a low atomic number ($Z = 6$). The minimum diameter of the x-ray beam measured at the focal spot is $4\,\mu$m, the opening angle of the radiation cone is approximately $160°$. A stable vacuum in the interior of the X-ray tube is created by a MVP 020-3 DC vacuum pump from Pfeiffer Vacuum while a water cooling system ensures temperature stability of the X-ray tube and target. The X-ray tube can be controlled directly with the X-Com program. The necessary steps to start the X-ray tube are described in chapter 6.1.

The CT-Alpha uses a large-area, low-noise CMOS detector to record radiograms. In comarison to a CCD detector, a CMOS detector has the advantage that pixels can be read out separately and not row by row. The C7942SK-25 detector from Hamamatsu provides 12-bit, so the brightness of a pixel is represented by $2^{12} = 4096$ different gray values. The detector has a size of $120 \times 120\,\text{mm}^2$ equivalent to 2400×2400 pixels where the pixel has a size of $50 \times 50\,\mu\text{m}^2$. The minimum adjustable integration time of the CMOS detector is 500 ms. A doped Gadolinium oxysulfide scintillator screen is placed in front of the CMOS detector to convert the incoming x-ray photons into visible photons which can be recorded by the CMOS detector.

Note: Due to the high-energy x-rays some pixels of the detector fail (bad pixel). The X-Tom control program is capable of detect inactive pixels and remove them from the image. This causes a slight reduction of the maximum resolution of the detector. Therefore, record the the current resolution of the detector when carrying out the experiment. This information is required to for a later evaluation of the images.

3. SAFETY INSTRUCTIONS

In the advanced experimental lab experiment „X-ray tomography "you will work with a scientific computer tomograph of significant financial value. To ensure a smooth and safe operation, the following instructions must be observed:

- Controlling the CT-Alpha via the *X-Tom* software must be done with care. The following section provides you with a brief introduction to the program. If you have any questions please contact the person responsible for the device!

- The CT-Alpha has a full lead housing and closing contacts that prevent the X-ray tube from being put into operation with the sliding door or channels open. Be careful when putting the X-ray tube into operation, always make sure that the safety circuit is actually closed. If the contacts are closed, the *Interlock* indicator in the program X-Tom light lights up green, see figure 4.1 on the left. If the indicator light lights up red, close the door completely with one strong pull. **It is strictly forbidden to bridge contacts!**

- During an experiment, a flashing red warning light in the housing of the CT-Alpha indicates that the X-ray tube is in operation. As long as this warning light is flashing, you must not open the sliding door of the CT-Alpha. The red emergency switch located on the outer housing of the CT-Alpha can be used to stop the CT-Alpha in case of an emergency. After completion of each experiment, switch off the voltage of the X-ray tube

(see start / stop X-ray tube). Only when the red warning light has stopped flashing, you can open the door of the CT-Alpha.

- Pay attention when setting acceleration voltage U and Anode current intensity I always ensures that the maximum power $P_{max} = U \cdot I$ is not exceeded. For each selected acceleration voltage and anode current check if the actual power is below the maximum power. The X-ray tube must be operated below the **maximum power of $P_{max} = 25\,\text{W}$!**

- During operation, the target and sample sometimes become very hot. Regard Make sure that you and the samples used before, during and Do not touch the target or the detector after the experiments.

- To prevent motion during a tomography scan, make sure to always fix your sample sufficiently.

4. The controlling software x-Tom

The CT-Alpha computer tomograph comprising the X-ray tube and the axes for positioning your sample are accesssible via the *X-Tom* control software. Below you will get to know the most important functions and commands of the software.

Figure 4.1 shows a full screen view of the X-Tom control software. The figure 4.2 and 4.3 provide an overview of the most important control panels that you will use during your experiments. **Please note: X-Tom must not be closed for the entire duration of the experiment. If you want to return to the desktop, just minimize the program.**

In the left window area, X-Tom displays a live image of the detector. The figure 4.1 shows an example of a radiogram of a surprise egg with a toy car enclosed. Use this radiogram to set the optimal sample position and, with the housing closed, the values for acceleration voltage, anode current and integration time. To the right, a histogram provides information about the gray values of the entire radiogram. You can use the *Profile* icon to select a line in the live image (in Figure 4.1 with red stitches) and the associated gray values can be output. In our example in Figure 4.1 you can see the metal axes of the toy car based on the two peaks in the line profile of the gray values. With the help of the histogram, the X-ray parameters can be further optimized to the greatest possible extent to generate measurement signal. You can also use the icon *Adjust* adjust the image contrast. This icon only changes that Display on the screen and does not change your raw data. At the You can do this with the icon *Axial CT* on the right edge of the X-Tom Open the *Manipulator* window as shown in Figure 4.3 is shown and explained below becomes:

In the *Manipulator* screen you can change the position of the sample stage in three spatial directions: left/right, down/up and forward/back. The sample table can also be rotated around its own axis. You carry out the test by entering the desired position in the white field and confirming with *enter*. The position of the detector is changed manually if necessary and cannot be moved automatically. At the beginning of the experiment, familiarize yourself with how to move the sample table in the desired spatial direction via the X-Tom. Attention: If you change the position of the detector, the sample stage can no longer be moved freely along
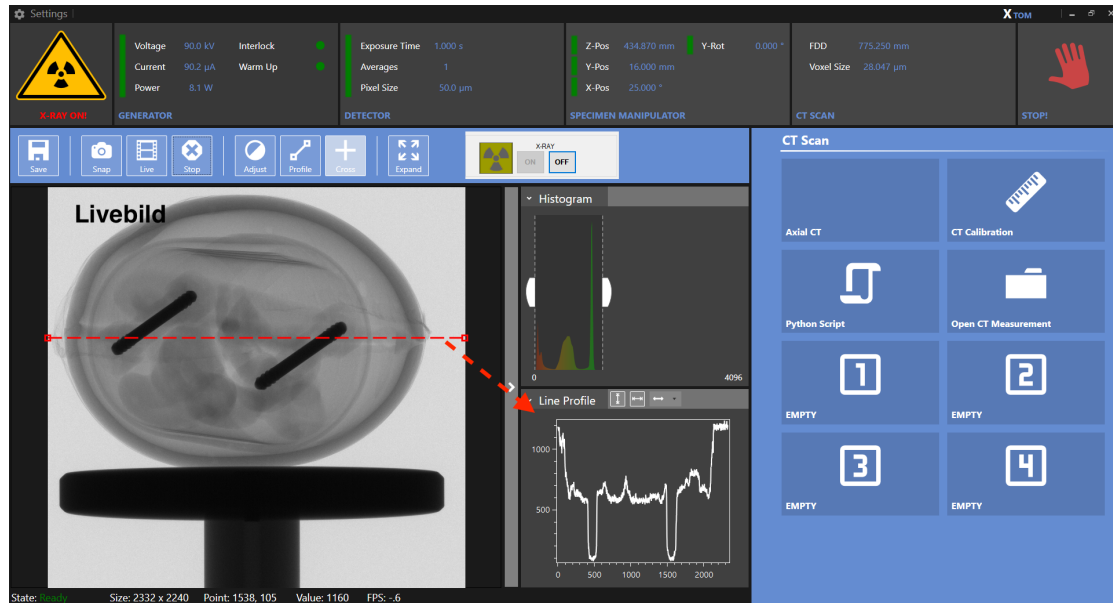
Figure 4.1: Overview of the main menu of the X-Tom program. A live image or snapshot of the intensity distribution (radiogram) can be displayed in the large left image field. To do this, you must click on the corresponding icon (*Live* or *Snap*) on the bar above the image area. Radiograms can be saved on the computer using the *Save* icon. With the icon *Live* you switch back to the live image, which can be stopped with the *Stop* icon. In the middle image fields, histograms of the gray values of the live image are displayed. On the right you mainly need the icon *Axial CT*; The window that opens when you click on it is shown in Fig. 4.3. With the icon *Open CT Measurement* you can select the folder in which you can save your measurements. If the device needs to be calibrated using the *CT Calibration* icon, carry this out together with the person responsible for the experiment.
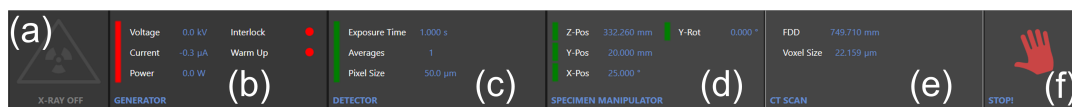

Figure 4.2: Status bar of the X-Tom program. Display from left to right: *(a)*: X-ray tube operating display. *(b)*: Current voltage, current and power of the X-ray tube. The "Interlock" and "Warmup" status indicators show whether the housing of the CT-alpha is closed (red: open, green: closed) and whether the X-ray tube is being warmed up/calibrated (red: CT is in warmup, green: Warmup was completed successfully). *(c)*: Detector settings, integration time in seconds, number of averages and size of pixels. *(d)*: position of the sample holder. *(e)*: Distance between source and detector (Focal-Detector Distance, FDD), size scale of the image in pixels/μm. *(f)*: stop button. (Clicking on the status fields (b)-(e) opens detailed menus in which the respective settings can be adjusted. These menus are shown in Fig. 4.3.)
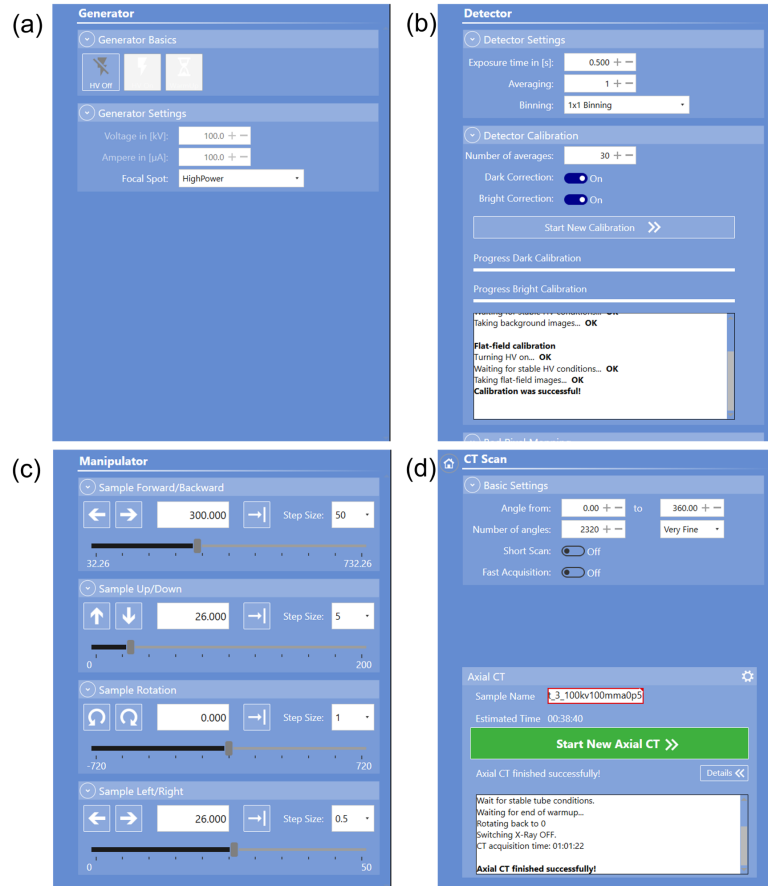
Figure 4.3: (a): Generator settings menu: voltage, current. Always use the HighPower mode as the focal spot. (b): Detector settings menu: Here you can set the exposure time. Note that the smallest adjustable time is 0.5 s. (c): Menu for axis control with the X-Tom program. "Sample Forward/Backward" corresponds to the z-axis in Fig. 2.1, "Sample Up/Down" to the y-axis and "Sample Left/Right" to the x-axis . Under the "Sample Rotation" option you can set the current rotation angle of the sample table. (d): CT scan: Here you can set the number of radiograms of a complete tomography.
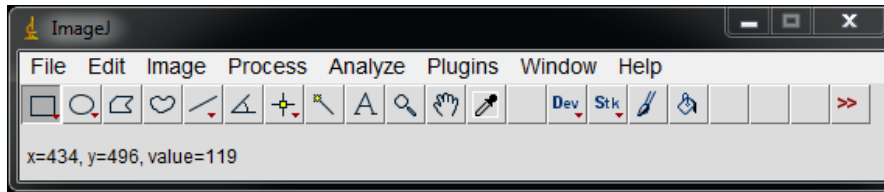
Figure 5.1: Overview of the image processing program ImageJ.

the z-axis. With the CT door open, check how far you can move the sample stage and note the maximum permitted positions of the sample stage. Never move the sample table beyond these positions!

5. IMAGE PROCESSING WITH IMAGEJ

The radiograms recorded in the X-Tom control program are saved in raw data format `*.raw`. To save your radiograms on the control computer, create a separate folder with your name in the *Fopra* folder. Save your radiograms separately according to tasks and name all radiograms in a meaningful and comprehensible way. Please remember to bring a USB stick with at least 4 GB of storage so that you can take your measurement data home with you for evaluation. Since the complete tomography file is usually larger than 2 GB, please make sure that your USB stick is formatted in FAT32 or NTFS.

For further processing of the radiograms in the raw data format `*.raw`, the image processing program *ImageJ* is used (see figure 5.1). You can download the installation file for this free of charge using the following link Download: `https://imagej.net/software/fiji/downloads`.

In the upper window area of ImageJ you will find various tabs for opening, editing, analyzing and saving images. To be able to read gray value information with ImageJ, import the radiograms in raw format using the settings shown in Figure 5.2. Images in `*.png` format do not need to be imported, but can be opened conventionally. In the middle window area of ImageJ, below the individual tabs, there are various shapes that can be used to mark areas within the opened image. At the bottom of the window, ImageJ indicates the position of your mouse pointer within an open image in pixels. In addition, the gray value belonging to the selected pixel is output (e.g. value=119).

ImageJ provides a number of options that can be used for data analysis. Using the *Plot Profile* option in the *Analyze* tab, ImageJ creates a gray value profile for the area of the image that you have marked in advance. The table belonging to the gray value profile can be exported and used for further analysis in a spreadsheet program, e.g. Origin. Using the *Histogram* option, which can also be found in the *Analyze* tab, a frequency distribution of the gray values (mean value and standard deviation) can be created over the previously selected image area. To begin evaluating your data, familiarize yourself with ImageJ and test the various options available to you using a selected radiogram.
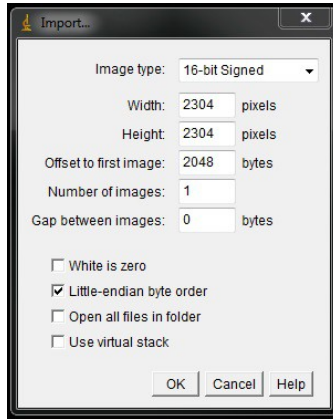
Figure 5.2: Example settings for importing raw files into ImageJ. Please note the exact values of the image width, height and offset that you use during the experiment so that you can display the images correctly for evaluation later.

6. EXPERIMENT

Document the following experiments in your experimental protocol and note the X-ray parameters used in each case. Since you will be recording a whole series of radiograms, you should save them in their own folders and name them in a meaningful and understandable way. You are welcome to take photos of the experimental setup and include them in your work. Your test protocol will also be part of the development.

6.1. PREPARING STEPS

Before starting the experiments, the X-ray tube of the CT-Alpha must be brought to operating temperature and the position of the electron beam must be calibrated. This "warm up" takes approximately 20 minutes. Remove all objects from the beam path, bring the detector into its final position and close the door of the CT-Alpha. Start a refresh in the X-COM program (see figure 6.1). The completion of the refresh after about five minutes is displayed in X-COM (Refresh ... done!). **Minimize X-COM, but do not close it!**

Note: Experimental setups by employees of the Seemann working group may limit the freedom of movement of the sample table within the CT-Alpha. Before starting the following parts of the experiment, decide on this together with the person responsible for the experiment, determine the limits within which you can move the detector on the magnification axis. Note the two limit positions found and only move the sample stage within these limits.

6.2. KRAMERS' RULE

Below you will check how the measured intensity, i.e. the measured gray values, depend on the anode current strength, the integration time and the applied voltage. Compare your mea-
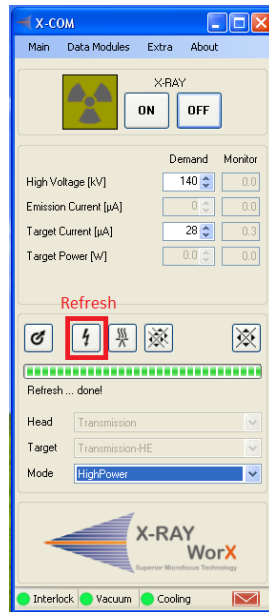
Figure 6.1: The Xcom program while starting a refresh.

surement results in this part of the task with your expectations from task 5 in the preparation questions. Discuss the significance of this part of the task with regard to the feasibility of a complete tomography.

6.2.1. DEPENDENCE OF THE INTENSITY ON THE ANODE CURRENT STRENGTH

For a medium acceleration voltage U, choose two different integration times below the saturation of the detector. If the integration time is fixed, vary it Anode current from $22.5\,\mu A$ up to the maximum current a power of $25\,W$ (calculate beforehand!) in steps of $22.5\,\mu A$ and take one frame at a time. Repeat the measurement for the second integration time. Ask both Show the series of measurements in a diagram and explain the curve shape you found. In general, before starting each series of measurements in this and the following experiments, you should check whether the radiogram has usable quality for the selected fixed X-ray parameters for both the largest and the smallest variable value.

6.2.2. DEPENDENCE OF INTENSITY ON INTEGRATION TIME

With the same acceleration voltage U as in the previous task, choose two different current intensities (note maximum power of $25\,W$) below the saturation of the detector. With a fixed current intensity, vary the integration time from $500\,ms$ to $1250\,ms$ in steps of $250\,ms$ and take one frame at a time. Repeat the measurement for the second current level. Display both series of measurements in a diagram and justify the curve you found using your calculations from the preparation questions.

With the same acceleration voltage, the gray values that were measured at different integration times or anode current intensities can be converted into one another. Match your measurement curves from the two previous parts of the task and justify your approach.

6.2.3. Dependence of the intensity on the anode voltage

Below you will examine the relationship between the gray values or the X-ray intensity and the acceleration voltage with a fixed anode current and integration time. With an integration time $t = 1\,\text{s}$, choose two different anode current strengths and vary the acceleration voltage from 20 kV to 110 kV in steps of 10 kV. For one of the two measurements, also carry out a control measurement by varying the acceleration voltage with the same X-ray parameters from 110 kV to 20 kV in steps of 10 kV downwards. Wear all three Display measurement curves graphically and discuss your measured values. Explain possible deviations.

6.3. Absorption of X-rays

Below you will determine the mass attenuation coefficient μ/ϱ of aluminum and carbon using radiogram images. You will receive a wedge made of aluminum and carbon from the person responsible for the experiment. First, estimate the density ϱ of the materials by determining the weight and volume of the wedges. Be careful with the wedges throughout the entire experiment; some materials are extremely easily deformed and can no longer be used for further measurements if they are damaged!

Set the CT parameters to a voltage of $U = 100\,\text{kV}$, a current of $I = 100\,\mu\text{A}$ and an integration time of $t = 1\,\text{s}$. Then first perform bright and dark field correction for these settings and then take a bright image. Think about what information you can get from this bright image. With regard to the results of the previous part of the task, discuss why you need the dark field correction.

Note: The dark image shows the image captured by the detector while the tube is turned off. It is used to correct the radiograms for the background noise of the detector. The bright image contains the information that the detector receives with a fixed power of the X-ray tube and a fixed integration time without an object in the beam path. With the help of the bright image, differences in pixel sensitivity and inhomogeneities in the beam path, which are caused, for example, by the conical beam path, are compensated for on the radiogram. The so-called bad pixel map contains information about which detector pixels need to be neglected or corrected when recording a radiogram because these pixels are defective or do not detect properly.

Now fix the two wedges on the sample table. Make sure that the long edge of the wedges is aligned along the light path and take a radiogram. Write down all the essential information (e.g. resolution, voxel size) that you need for your evaluation.

Repeat your measurements after you and your person responsible for the experiment have installed a copper filter in front of the X-ray source. For this measurement, increase the integration time to $t = 7\,\text{s}$. The voltage and current do not need to be changed. Here too, first carry out bright and dark field correction and take a bright image.

Carry out the following evaluation for the radiograms of the two wedges recorded with and without a copper filter. Using ImageJ and the *Plot Profile* function, determine the gray values along a vertical line for both wedges. The gray values correspond to the measured intensity J on the screen. Determine the logarithm $ln(J(x)/J_0)$ of the ratio of the measured intensity $J(x)$ to the initial intensity J_0 and plot your values graphically as a function of the absorber thickness x. Use Lambert-Beer's law (1.9) to discuss what course you expect. Approximate the data points using a suitable compensation function and use this to determine the attenuation coefficients μ for aluminum and copper. By dividing these values by the previously determined densities, you get the respective mass attenuation coefficient μ/ϱ. Compare your events to the literature values of the mass attenuation coefficient `https://physics.nist.gov/PhysRefData/XrayMassCoef/tab3.html`. In this context, discuss the role of the copper filter.

Note: With the given CT parameters you should theoretically achieve a photon energy of $E = 100\,keV$. In fact, this value is the maximum energy of the emitted photons and the typical energy of the photons is significantly lower. The maximum distribution of photon energies corresponds to approximately $60\,keV$ for the CT parameters used.

6.4. DETERMINATION OF SPHERICAL ARRANGEMENTS USING RADIOGRAMS

For the following part of the experiment, the person responsible for the experiment will provide you with a plastic block that is not transparent to the human eye and contains several layers of balls in different arrangements. The balls all have the same diameter, but can be made of different materials. Determine the respective arrangement of the spheres by taking radiograms of the plastic block at different angles (e.g. 0°, 45°, 90°, 135°).

Orient the plastic block on the sample stage so that the arrow points toward the X-ray source. First set your test parameters (current, voltage, integration time) for optimal contrast. Use the same settings for all measurements (including the initial test shots).

Tip: The balls are not arranged randomly, but are all arranged on regular grids (in a square, hexagonal or circular arrangement). However, some orders deliberately left vacant positions. At the beginning of this task you will receive "empty" plastic blocks with the basic patterns and balls made of the different materials used to determine the attenuation of the X-rays within the plastic block or the balls made of the different materials. Using ImageJ and the Plot Profile function, you can evaluate the intensity of the X-rays in your radiograms to determine the sphere arrangement and the sphere material.

6.5. COMPLETE COMPUTED TOMOGRAPHY

The person responsible for the experiment will give you a sample for the following part of the experiment, which you will examine using X-ray tomography. The sample consists of several layers of aluminum blocks enclosed in a plastic block, the arrangements of which have irregular gaps. The different layers also have different heights. First, analogous to the previous part of the experiment, try to see whether you can make a statement about the arrangement

and "layer thickness" of the aluminum cuboids by taking a few radiograms at different angles. Then take a complete tomography of the plastic block.

To do this, mount the plastic block (and, if necessary, an object of your choice) on the sample holder together with the person responsible for the experiment, close the CT and start the X-ray tube. Align the sample in the beam path and set the X-ray parameters so that the live image has sufficiently good contrast. Discuss with the person responsible for the experiment whether the recording parameters you have chosen make sense. After you have made all the settings, you are not allowed to change anything in the sample position or in the X-ray parameters! Check whether there is a light and a dark image for the parameters you have selected. If not, remove the sample from the beam path and take the missing correction image.

Finally, start the tomography. You can carry out the reconstruction of the tomography together with the person responsible for the experiment. The program *VGStudio* is used for this purpose on the PC set up next to the control computer. Open any tomogram of your sample in *VGStudio*. Together with the person responsible for the experiment, select the area to be reconstructed, mark the so-called *IO area* and start the reconstruction. Using your 3D reconstruction of your sample, make horizontal sections showing the arrangement of the aluminum cuboids. Using the reconstructed data, also determine the respective „layer height ".

7. NOTES ON THE ELABORATION

The final elaboration represents an essential part of every attempt in the advanced internship and should be viewed as a practice opportunity with a view to later final theses. Your elaboration should therefore be written in the style of a scientific paper and only contain comprehensible or verifiable statements. The elaboration includes a title page, a table of contents, an introduction, a summary and an overview of the literature and illustrations used. You should also include your test protocol in the appendix to the report. All chapters should begin with a few introductory sentences and end with a brief summary. Make sure that the subheadings and headings of figures and tables are correct and refer to them in the running text. Include relevant information, such as x-ray parameters used, in image captions and scale images where necessary. Explain mathematical explanations and thought processes with sketches and comment on your explanations so that you can understand your elaboration even without knowledge of the experiment instructions. Comment on your results, question them and evaluate them. Last but not least, pay attention to the use of standard language and compliance with the rules of German spelling.

REFERENCES

[1] Dieter Meschede. *Gerthsen physik*. Springer-Verlag, 2015.

[2] H. A. Kramers. Xciii. on the theory of x-ray absorption and of the continuous x-ray spectrum. *The London, Edinburgh, and Dublin Philosophical Magazine and Journal of Science*, 46(275):836–871, 1923.

[3] Avinash C Kak and Malcolm Slaney. *Principles of computerized tomographic imaging*. SIAM, 2001.

A. Reconstruction algorithms

The laws discussed so far allow conclusions to be drawn about the structure and material of homogeneous three-dimensional objects via the local distribution of the attenuation coefficient μ(x,y) in radiograms. However, the information from a single two-dimensional radiogram is not sufficient to determine the internal structure of complex (inhomogeneous) three-dimensional objects. What is needed here is a series of radiograms (projections) that were recorded from different projection angles.

In order to calculate a three-dimensional image, complex reconstruction algorithms are necessary, the basic principle of which will be outlined below. For the sake of simplicity, in the context of this experimental procedure we consider the reconstruction of two-dimensional images from n projections that were recorded at different projection angles θ relative to the x-axis. Figure A.1(a) shows two pixel points as the simplest example; The blue dashed lines symbolize a group of projection lines at the angle θ, which can be assumed to be parallel to each other. In Cartesian coordinates, the line integral along each projection of this two-dimensional image can be represented with the function f(x,y), which gives the distribution of the attenuation coefficients. Using a so-called Radon transformation, the coordinate system can be rotated counterclockwise by θ and converted into the polar coordinate system (s,t). The following applies:

$$t = x\cos\theta + y\sin\theta$$
$$s = -x\sin\theta + y\cos\theta \tag{A.1}$$

The Radon transformation p(s,θ) of a distribution function f(x,y) with the transformation operator $\mathscr{R}$ is given by:

$$\mathscr{R}f(s,\theta) = p(s,\theta) = \int_{-\infty}^{\infty}\int_{-\infty}^{\infty} f(x,y)\cdot\delta(x\cos\theta + y\sin\theta - s))dxdy$$
$$= \int_{-\infty}^{\infty} f(s\cos\theta - t\sin\theta, s\sin\theta + t\cos\theta)dt \tag{A.2}$$

Equation A.2 shows that the integrand limits the function values of f(x,y) to a line ($x\cos\theta + y\sin\theta - s = 0$). For a two-dimensional image, this corresponds to an absorption image along a specific line. For different projection angles θ we get a straight line in polar coordinates for the central pixel in Fig. A.1(a) and a curve for the pixel at the top right as in Fig. A.1 (b) shown. This type of representation is called a *sinogram*.

In order to make the original image visible, a back transformation into the Cartesian coordinate system (x,y) is necessary, which is explained using a more complex example. Figure A.2 shows the coat of arms of our university A.2(a) and the associated sinogram A.2(b). With a direct rear projection

$$\tilde{f}(x,y) = \int_0^{\pi} p(s,\theta)|_{s=x\cos\theta + y\sin\theta}d\theta \tag{A.3}$$

the image can be reconstructed based on a different number n of projections, as shown in Fig. A.3. It is clearly visible that the reconstructed images are blurry using the direct projection method, regardless of the number of projections used for reconstruction.
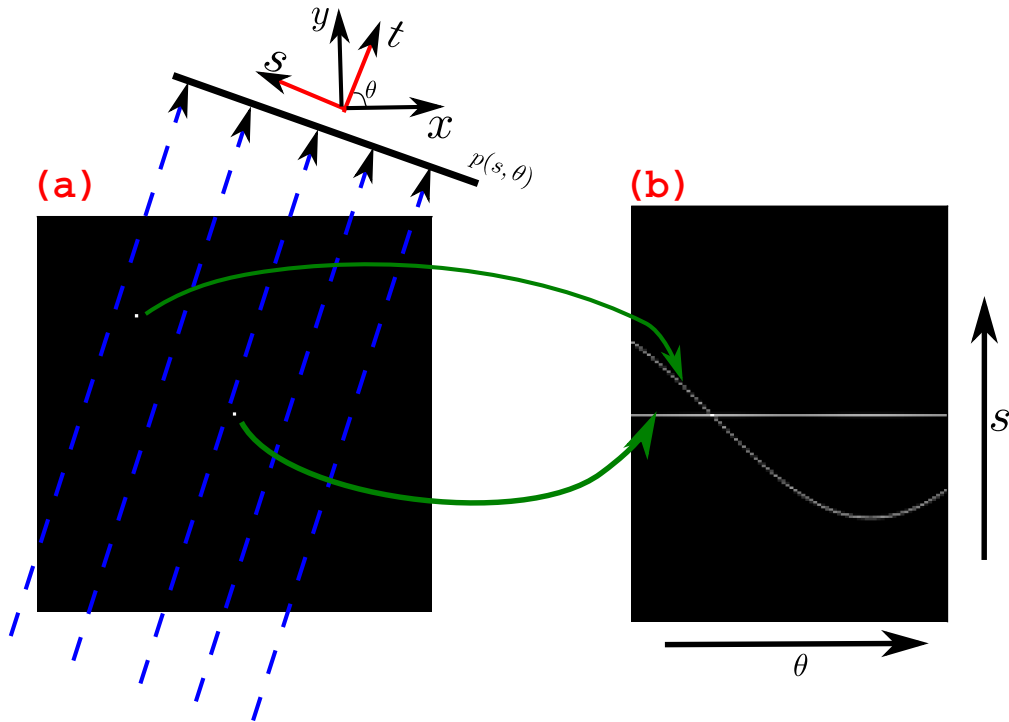
Figure A.1: (a) Original image of two pixels; (b) Radon transform of the two pixels in (a).
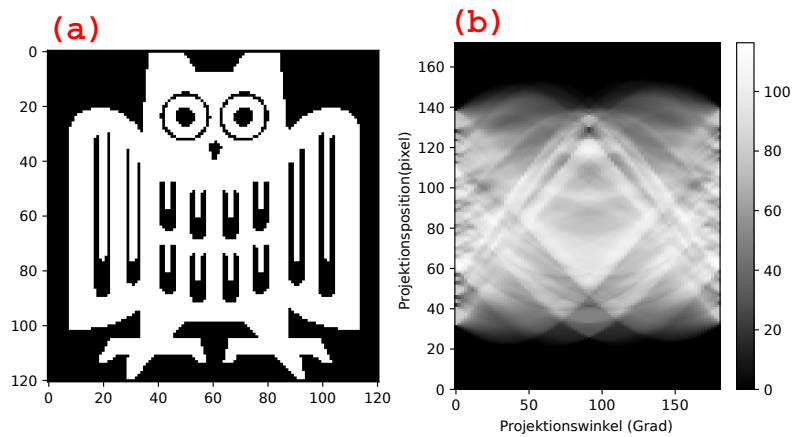

Figure A.2: (a) original images; (b) Radon transformation of (a).

The underlying problem lies in the conversion from polar to Cartesian coordinates. The polar coordinates are primarily introduced into the transformation to facilitate the calculation simplify. The problem appears when switching from polar to Cartesian coordinates because they cannot match exactly. In the polar coordinate system, the values in the area of the origin are closer to each other and spread out in space with increasing distance from the origin. This leads to blurring, which can be seen in rear projection without filtering. Direct
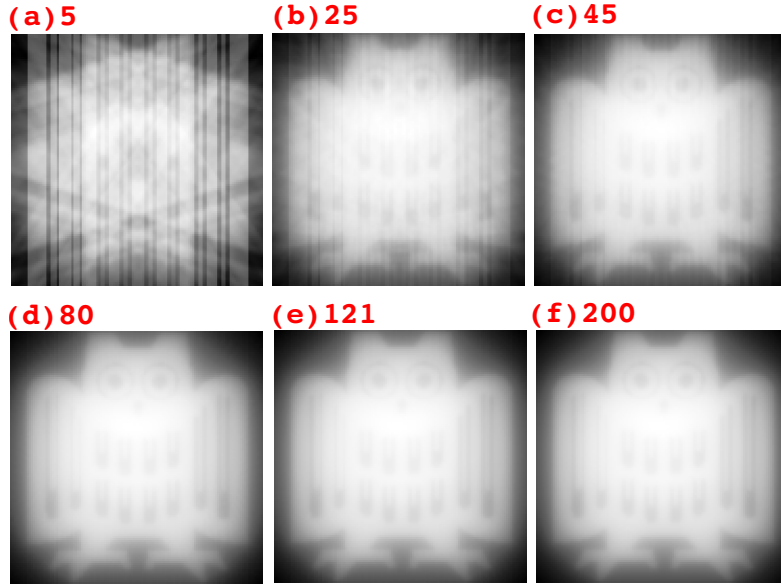
Figure A.3: Reconstructed images with different numbers of projections.

back projection therefore only leads to an unsatisfactory result and inverse back projection is usually used for image reconstruction. The two most commonly used ways to invert the Radon transformation are the *Fourier slice theorem* and the *filtered back projection*, the basic principles of which are briefly explained below.

In both the Fourier slice theorem and the filtered back projection, the Radon transform is inverted using a Fourier transform. Assuming that the Fourier transform of $p(s, \theta)$ over the variable s $P(\omega, \theta)$ gives:

$$
\begin{aligned}
P(\omega, \theta) &= \int_{-\infty}^{\infty} p(s, \theta) e^{-i2\pi\omega s} ds \\
&= \int_{-\infty}^{\infty} \int_{-\infty}^{\infty} f(t\cos\theta - s\sin\theta, t\sin\theta + s\cos\ theta) Germane^{-i2\pi\omega s} ds
\end{aligned}
\tag{A.4}
$$

where with equation A.1:

$$
dsdt = \begin{vmatrix} \cos\theta & -\sin\theta \\ \sin\theta & \cos\theta \end{vmatrix} dxdy = dxdy
\tag{A.5}
$$

With the equations A.4 and A.5, the Fourier transformation then has $P(\omega, \theta)$,

$$
\begin{aligned}
P(\omega, \theta) &= \int_{-\infty}^{\infty} \int_{-\infty}^{\infty} f(s\cos\theta - t\sin\theta, s\sin\theta + t\cos\ theta) dt e^{-i2\pi\omega s} ds \\
&= \int_{-\infty}^{\infty} \int_{-\infty}^{\infty} f(x, y) e^{-i2\pi\omega(-x\sin\theta + y\cos\theta)} dxdy
\end{aligned}
\tag{A.6}
$$

If we perform a direct Fourier transformation of the original image f(x,y) then:

$$
F(u, v) = \int_{-\infty}^{\infty} \int_{-\infty}^{\infty} f(x, y) e^{-i2\pi(xu + yv)} dxdy
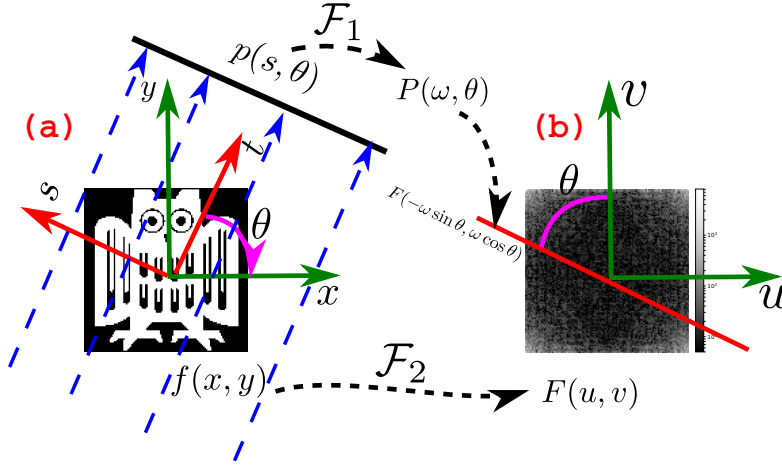\tag{A.7}
$$

Figure A.4: Illustration of the Fourier slice theorem.

If you compare equation A.6 and equation A.7, according to the Fourier slice theorem [3]:

$$F(-\omega\sin\theta, \omega\cos\theta) = P(\omega, \theta) \tag{A.8}$$

The parametric curve $(u = \omega\sin\theta, v = \omega\cos\theta)$ describes a line that passes through the zero point in Fourier space, as in Fig.A.4(b) shown. The angle between the cut $F(-\omega\sin\theta, \omega\cos\theta)$ and the u axis in Fig.A.4(a) is the same as the angle between the projected profile $p(s, \theta)$ and the x-axis in Fig.A.4(b). In short, the Fourier transform of the projection of an object at a certain angle corresponds to a line in the same direction of the two-dimensional Fourier transform of the same object. If we collect enough projections we can fill the Fourier space. With an inverse Fourier transform we can complete the task of reconstruction.

Theoretically, under ideal conditions, a perfect image can be created using the Fourier slice theorem. However, if we apply the Fourier transform for each projection to fill the Fourier space, we immediately notice that the region near the zero point in Fig.A.4(b) has more sampled points . Image reconstruction using the Fourier slice theorem is very computationally intensive and error-prone, which continues to result in a blurry image. This problem can be solved using filtered back projection, the algorithm of which is now presented.

The original image or object defined as $f(x, y)$ can be calculated using the inverse Fourier transform:

$$f(x, y) = \int_{-\infty}^{\infty}\int_{-\infty}^{\infty} F(u, v)e^{i2\pi(ux+vy)}dudv \tag{A.9}$$

Starting from equation A.8, we assume that $u = -\omega\sin\theta, v = \omega\cos\theta$, which means:

$$dudv = \begin{vmatrix} -\sin\theta & -w\cos\theta \\ \cos\theta & -w\sin\theta \end{vmatrix}d\omega d\theta = \omega d\omega d\theta \tag{A.10}$$

With the equations A.9 and A.10 we get:

$$f(x, y) = \int_{0}^{2\pi}d\theta\int_{0}^{\infty} F(-\omega\sin\theta, \omega\cos\theta)e^{i2\pi\omega(-x\sin\theta+y\cos\theta)}\omega d\omega \tag{A.11}$$

If you replace $F(-\omega\sin\theta, \omega\cos\theta)$ according to the Fourier slicetheorem by $P(\omega, \theta)$ according to Eq.A.8, this is how you get:

$$f(x,y) = \int_0^{2\pi} d\theta \int_0^{\infty} P(\omega,\theta) e^{i2\pi\omega(-x\sin\theta+y\cos\theta)} \omega d\omega$$
$$= \int_0^{\pi} \int_{-\infty}^{\infty} P(\omega,\theta) |\omega| e^{i2\pi\omega s} d\omega d\theta \tag{A.12}$$

$|\omega|$ in Eq. A.12 produces a convolution in Fourier space and thus a filtering in spatial space. So the Fourier transform $P(\omega,\theta)$ is filtered by the frequency range $|\omega|$ before we perform the inverse Fourier transform. Using this method, we obtain the filtered back projection with a sharp image of the original image, as shown in Fig.A.5. Finally, it should be mentioned that the term $|\omega|$ can also be replaced by other expressions to obtain alternative filtering. The initial approximation that the incident beams are parallel to each other is not permitted for systems such as the X-ray tomograph used in this experiment. In our case, the radiation is emitted conically from the X-ray source and the actual image reconstruction algorithms are more complex.
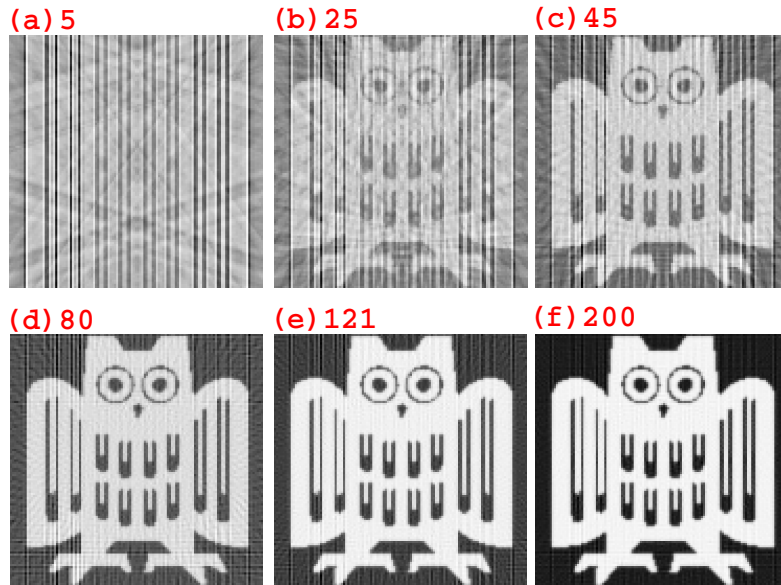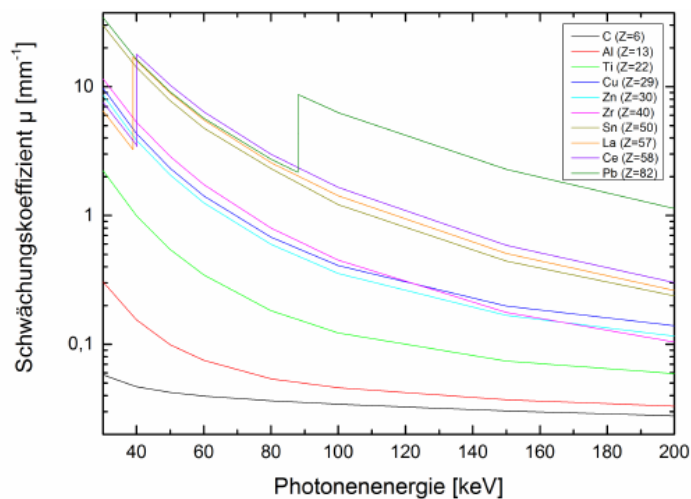

Figure A.5: Reconstructed images with different numbers of projections (filtered back projection, ramp).

B. ATTENUATION COEFFICIENTS

Figure B.1 gives an overview of the attenuation coefficients μ of the materials carbon (Z=6), aluminum (Z=13), titanium (Z=22), copper (Z=29), zinc (Z=30), zirconium (Z=40), tin (Z=50), lanthanum (Z=57), cerium (Z=58) and lead (Z=82) as a function of photon energy.

Energie keV	μ mm^{-1} C (Z=6)	μ mm^{-1} Al (Z=13)	μ mm^{-1} Ti (Z=22)	μ mm^{-1} Cu (Z=29)	μ mm^{-1} Zn (Z=30)	μ mm^{-1} Zr (Z=40)	μ mm^{-1} Sn (Z=50)	μ mm^{-1} La (Z=57)	μ mm^{-1} Ce (Z=58)	μ mm^{-1} Pb (Z=82)
30	0,0579	0,3046	2,2374	9,7406	8,618	11,5553	29,9391	6,4908	7,579	34,3889
38,9246								3,2522		
38,9246								17,1032		
40	0,0465	0,155	0,9963	4,3369	3,8442	5,2964	14,1086	16,0235	3,5321	16,2871
40,0443									3,4312	
40,0443									17,8469	
50	0,0423	0,099	0,5459	2,3308	2,0649	2,8704	7,7736	8,928	10,295	9,1201
60	0,0396	0,075	0,3447	1,421	1,2566	1,741	4,7687	5,5296	6,3985	5,6948
80	0,0364	0,054	0,1823	0,6806	0,5972	0,8003	2,3172	2,5772	2,9862	2,7436
88,0045										2,1663
88,0045										8,7141
100	0,0342	0,046	0,1224	0,4089	0,3551	0,4491	1,2176	1,4284	1,656	6,2937
150	0,0304	0,037	0,0742	0,1978	0,1671	0,1762	0,4425	0,5083	0,5884	2,2843
200	0,0278	0,033	0,0591	0,1391	0,1155	0,104	0,2368	0,2615	0,3015	1,1325

Figure B.1: Attenuation coefficient μ as a function of photon energy for various materials (Source: http://www.nist.gov/pml/data/xraycoef/index.cfm)